JOURNAL OF CATALYSIS 144, 160–174 (1993)

Selective Reduction of Diphenyldisulfides Catalysed by Sulfides—Influence of the Nature of the Catalyst

CHRISTOPHE CALAIS, MICHEL LACROIX, CHRISTOPHE GEANTET, AND MICHÈLE BREYSSE

Institut de Recherches sur la Catalyse, 2 avenue Albert Einstein, 69626 Villeurbanne Cedex, France

Received December 15, 1992; revised April 14, 1993

The catalytic activities of a series of sulfide catalysts have been examined for the reduction of diphenyldisulfide into benzenethiol. This reaction was studied in a gas–liquid–solid batch reactor. The first step of this study was devoted to the hydrodynamic of the reactor in order to ensure that the reaction proceeds under chemical control. The catalytic activities of the various catalysts vary in a wide range, the most efficient being one of the industrial hydrotreating catalyst tested, i.e., a $NiMo/Al_2O_3$. Whatever the nature of the active phase, the reaction was 100% selective toward the formation of benzenethiol. The effects of reducing pretreatments on the catalytic activities as well as the results of TPR and TPD studies suggest reaction mechanism in which M–H (M = transition metal ion) and SH groups intervene simultaneously. © 1993 Academic Press, Inc.

INTRODUCTION

The most important metal sulfide catalysts are based on a Group VI metal such as molybdenum or tungsten promoted with a Group VIII metal (cobalt or nickel) generally supported on a gamma-alumina. The principal benefit of these catalysts is their ability to effect hydrogenation and carbon–heteroatom hydrogenolysis while being highly resistant to sulfur poisoning. This important property explains why the dominant use of these systems is for petroleum refining. However, beside this industrial aspect, several papers or patents have demonstrated that sulfide catalysts may present interesting properties in other reactions than those relevant to hydrotreatment. For instance, Weisser and Landa (*1*) have reported that the catalytic thiolation of ketones, aldehydes, alcohols, and nitriles, as well as the synthesis of mercaptans by addition of H_2S on an unsaturated C–C bond or the synthesis of amines by direct amination of alcohols, can be catalysed over sulfides. More recently, molybdenum sulfide has been applied in the selective conversion of carbon monoxide into hydrocarbons (*2*) or alcohols (*3–4*), and several patents have claimed the use of transition metal sulfides for the preparation of unsaturated amines by selective hydrogenation of nitro aromatics with acetylenic (*5, 6*) or ethylenic groups (*7*). Similarly, the transformation of chloronitrobenzenes into the corresponding anilines may be successfully achieved at moderate temperatures over conventional sulfided NiMo or CoMo hydrotreating catalysts (*8*). Recently, Malz and Greenfield have studied the preparation of tertiary aliphatic amines by reductive alkylation of dialkyl amines and that of alicyclic secondary amines with ketones in presence of hydrogen over various catalysts (*9*). Their results have nicely demonstrated that sulfide catalysts may present higher activities and selectivities than metals, particularly when sterically hindered ketones and amines are used as starting reagents.

Beside these applications of sulfide catalysts in fine chemical synthesis, some others can be foreseen, particularly in areas where the nature of feedstocks or reactants is such that rapid poisoning of other, more active

0021-9517/93 $5.00

catalysts would occur. For instance, such utilizations may be envisaged for the manufacture of pharmaceuticals or specialty chemicals having one or more sulfur atoms in their structures. Nevertheless, very few results dealing with thiochemistry have been reported in the literature since transition metal sulfides have been utilized for the selective splitting of organic sulfides into mercaptans (*10, 11*) or the dehydrogenation of thiacyclopentane into thiophene (*12, 13*).

Industrially, thiochemistry is related to the synthesis of about 30 compounds including mercaptans, sulfides, polysulfides, sulfones or sulfoxides, thioacids, and thioesters which are used in increasing quantities in agrochemicals, pharmaceutical products, petrochemicals, lubricants, cosmetics, and gas odorants. Among them, mercaptans are the most important because they are very often used as starting materials for the synthesis of the other thiocompounds. The synthesis of aliphatic mercaptans is currently achieved by direct thiolation of alcohols or through olefin reactions with H_2S. Both reactions are respectively catalysed by alkali metal salts or oxides supported on alumina and acidic catalysts (*14*). On such catalytic systems, mercaptan selectivities higher than 95% are generally obtained even for an almost complete conversion of the starting alcohol or olefin. In contrast to the preparation of aliphatic thiols, the synthesis of aromatic mercaptans seems to be less optimized. For instance, lower selectivities and conversions have been reported for the catalytic thiolation of phenol into benzenethiol (*15, 16*). Similar results were obtained with a mixture of chlorobenzene and H_2S (*17, 20*) or of cyclohexane and sulfur or sulfur chloride (*21*), or by dehydrogenation of cyclohexylmercaptan (*22*). The lack of selectivities observed in these catalytic reactions is probably related to the high temperatures and pressures needed for the transformation of these reactants. The methods now in favor for the synthesis of such thiols are reduction reactions which can be carried out under mild conditions, i.e., reduction of the corresponding sulfonic acids (*23–26*) or sulfonyl chlorides (*27–30*) with phosphorus or native hydrogen being produced with a metal and a mineral acid. If high selectivities could be observed (90%), such procedures would suffer from the disadvantage of forming large amount of phosphoric acid or metal chloride wastes. From literature data (*31–39*) it is also known that aryl thiols may be prepared by reducing the corresponding disulfides because the reverse reaction (conversion of thiols to disulfides) is a convenient protecting group technique used in organic synthesis. Moreover, the tertiary structure of a large number of proteins is strongly influenced by the S–S bond present in them. Consequently, the selective reduction of the disulfide linkage to thiols has been extensively studied from both chemical and biological viewpoints. These studies have been performed using nucleophilic reagents such as hydrides (*31–33*), trivalent phosphorus compounds (*34–36*), or hydroxide, cyanide, or hydrogen selenide ions (*35, 37*), as well as hydrazine derivatives (*38, 39*). Results reported in these works evidenced that S–S bond cleavage led exclusively to thiols and thiolates. However, it should be underlined that the involved reactions do not proceed catalytically since the co-reactants are consumed during the reaction course. Consequently, there is a need to develop catalytic processes working under mild conditions which will allow this selective reduction.

In the framework of a general study devoted to the examination of the properties of transition metal sulfides for reactions relevant to thiochemistry, we were interested first in a dehydrogenation reaction, i.e., the conversion of thiacylopentane into thiophene (*12, 13*), and then in a S–S bond cleavage, i.e., the reduction of diphenyldisulfide into benzenethiol. Both reactions are totally different from classical hydrodesulfurization since they do not imply sulfur removal but a dehydrogenation

in the first case and a S–S bond cleavage in the second case. The comparison of the properties of unsupported transition metal sulfides for the dehydrogenation of thiacyclopentane led to results close to those obtained for the hydrodesulfurization of thiophene. This suggested that the catalytic sites involved in both reactions are comparable (*12*).

The objective of the present work is to examine the properties of transition metal sulfides for the reduction of diphenyldisulfide. However, since this reaction was not carried out in the gas phase, as is usual for hydrodesulfurization or hydrogenation model reactions, but in the liquid phase, it appeared preferable to use supported catalysts. As a matter of fact, compared to unsupported ones, supported catalysts have higher mechanical resistances which is an important parameter when a mechanically stirred reactor is used. Furthermore, the utilization of supported catalysts having identical granulometry avoids any different behaviour with regard to additional internal diffusion problems. The active phases studied were the conventional CoMo, NiMo, and NiW mixed catalysts, as well as the corresponding unicomponent catalysts, i.e., Co, Ni, Mo, and W sulfides supported on alumina. Moreover, two additional phases were selected (Ru and Rh sulfides) since they were found to be highly active for C–S and C–N bond cleavage reactions. The activity scale, obtained for these various catalysts, in the reduction of diphenyldisulfide is compared to that observed for an aromatic hydrogenation test. The results are discussed in relation to TPR and TPD solid characterizations which give some indications about the nature of the active sites involved in the reduction of diphenyldisulfide. These reaction studies were carried out in a gas–liquid–solid reactor. Particular attention was paid to the hydrodynamics of the reactor and to the studies of the experimental conditions which make it possible to avoid mass transfer limitations.

TABLE 1

Catalyst Compositions

Metal	Concentrations	
	wt%	(10^{-4} mol/$g_{catalyst}$)
Ni	2.4	4.0
Co	2.4	4.0
Mo	9.3	9.7
W	16.6	9.0
Ru	7.7	7.6
Rh	8.0	7.8
NiMo	Ni : 2.4	4.0
	Mo : 9.3	9.7
NiW	Ni : 2.5	4.0
	W : 16.6	9.0
CoMo	Co : 2.4	4.0
	Mo : 9.3	9.7

EXPERIMENTAL

A. Catalysts and Materials

The CoMo, NiMo, and NiW catalysts were conventional industrial catalysts. For comparison purposes, the properties of Mo, W, Co, and Ni supported on alumina were also studied. These catalysts contain the same amount of the various transition metal sulfides as the mixed catalysts and they were prepared using the same support, i.e., a high surface area γ-alumina (S = 256 $m^2\ g^{-1}$, pore volume 0.61 $cm^3\ g^{-1}$). Prior to the sulfidation process, the catalysts were crushed and sieved to an average particle size of 100 μm (80–120 μm). Rhodium and ruthenium catalysts were prepared by the pore filling method using the same alumina (crushed and sieved to the same size as above). For these impregnations solutions of $RhCl_3$ and $RuCl_3$ were utilized. The various catalysts as well as their compositions are given in Table 1.

The catalysts were sulfided in a flow reactor at 673 K for 4 h in a 15% H_2S–85% H_2 mixture, except for the rhodium and ruthenium catalysts, which were sulfided in a 15% H_2S–85% N_2 atmosphere. As a matter of fact, previous studies carried out in our lab-

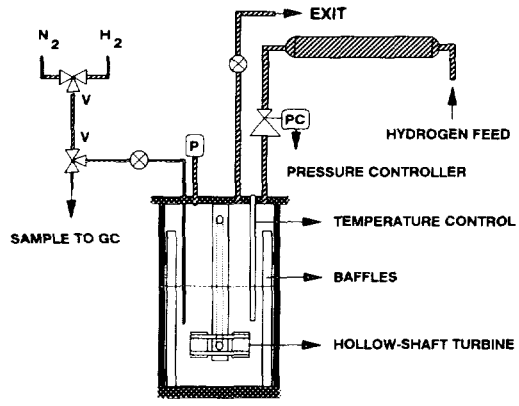

FIG. 1. Schematic representation of the batch reactor.

oratory showed that hydrogen should not be utilized in the sulfiding mixture to avoid the intermediate formation of a metallic state very difficult to sulfide afterwards.

For comparison purpose, three unsupported samples were also studied, MoS_2, RuS_2 and NiMoS. Their preparations were described in previous papers (*40, 41*). Their surface area measured by the BET method are respectively: 56, 70 and 15 $m^2 g^{-1}$.

After sulfidation, the samples were flushed with a N_2 flow and stored under argon in sealed bottles to prevent their oxidation. Diphenyldisulfide (DPDS), *n*-dodecane and *n*-tridecane (internal standard) were purchased from Aldrich (purity > 99%) and used without any further purification. Hydrogen used for catalytical runs was a high purity gas (99.995%) from Air Liquide.

B. Description of the Hydrogenation Reactor

The reactor used for catalytical tests is a 200 cm^3 stirred slurry tank reactor (STR) operating in a batch mode (see typical procedure). The scheme of the apparatus is given on Fig. 1. The autoclave is equipped with a hollow-shaft 6-bladed magnetically driven turbine with four baffles on the wall of the reactor to prevent vortex formation. This kind of stirrer makes it possible to obtain a very good dispersion of the gas into the liquid phase due to the aspiration which takes place when the rotation of the turbine creates a low pressure area in its center. The geometry of the reactor (e.g., baffles and blade sizes, diameter and position of the turbine, and height of liquid) was optimized (see Fig. 1) according to classical design to "perfectly mixed" triphasic reactors (*42*). At fast stirring rates, the gas hold-up ε, defined as the ratio $\varepsilon = V_g/(V_g + V_l)$ (V_g: gas volume dispersed into liquid, V_l: liquid volume) can be high ($\varepsilon = 0.15$ at 1500 rpm), which provides a high gas/liquid (G/L) interfacial area and consequently increases the overall G/L mass transfer rate, often limiting in three phase reactors. The system for sampling consists of a $\frac{1}{16}$-in. diameter tube such that the dead volume is minimized (0.4–0.5 cm^3). A set of two 3-port valves V allows this dead volume to be purged with H_2 (or N_2) before and after sampling. Hydrogen is introduced into the reactor through a pressure controller (PC) which makes it possible to maintain a constant pressure during the course of the experiment (working pressure interval 1–35 bar).

C. Typical Experimental Procedure

Catalytic runs were carried out in the reactor described above. In each run, the autoclave is charged with 5.0 g of DPDS dissolved in 75 cm^3 of *n*-dodecane (0.3 *M* solution) with a small amount (0.1 to 0.2 g) of *n*-tridecane used as an internal standard for the GC analysis. Freshly sulfided catalyst (0.1 g) was then added to the solution. The reactor was flushed with nitrogen and heated to the reaction temperature. Nitrogen was then replaced by a hydrogen atmosphere (3 bar) and the stirring was started. This step defines the zero time of the reaction. Samples (0.4–0.5 cm^3) were periodically withdrawn during the reaction course. Taking into account that less than 10 samplings were necessary to describe the kinetic curves, the volume of solution withdrawn

was then negligible. Analyses were performed on a HP 5890 A gas chromatograph equipped with a FID detector and with a nonpolar semicapillary column (HP-1 methyl silicon gum, 5 m × 0.53 mm, film thickness 0.23 μm), at a temperature programmed from 313 K to 523 K (15 K/min). Conversions were calculated either from the disappearance of DPDS or the formation of the products.

D. TPR and TPD Experiments

The temperature programmed reductions were carried out in conventional TPR equipment. An UV photodetector was employed to measure H_2S production. The detector was previously calibrated with a well-defined composition mixture containing 0.1% H_2S in H_2. The amounts of H_2S produced were obtained by the integration of the UV photodetector signal. The sulfided catalysts were kept under a flow of nitrogen at room temperature until no residual H_2S signal was detected. Nitrogen was replaced by a H_2 flow (100 cm^3/min for unsupported samples and 40 cm^3/min for supported catalysts) at atmospheric pressure and the temperature raised to 1070 K (2 K/min).

The flash desorption experiments were performed in the same apparatus under a nitrogen flow. A chromatograph equipped with a TCD detector allowed the measurement of the quantities of adsorbed H_2 and the UV photodetector those of H_2S. Preliminary experiments have shown that at moderate heating rates ($\approx$10 K/min) the obtained thermodesorption profiles were extremely large, indicating the presence of several chemisorbed species. In order to improve the resolution of the various peaks higher heating rates were used. For this purpose, the temperature of the catalyst was increased suddenly by introducing it into a furnace preheated to 573 K. A calculator–integrator allowed the simultaneous storage of the H_2 signal coming from the detector and measurement of the temperature of the catalyst bed.

RESULTS AND DISCUSSION

In heterogeneous catalysis, the specific activity is often the first measurement used to characterize a given catalytic material. However, such determination implies that the catalytic test is conducted under experimental conditions allowing chemical control of the reaction. If this could be easily achieved in solid–gas reactors, the use of G/L/S reactors may lead to significant mass transfer limitations due to the simultaneous presence of the gas, liquid, and solid phases. Therefore, the overall rate of the process (e.g., the measured rate, r) depends not only on the surface reaction rate but also on the G/L and L/S mass transfer rates (*43*). By definition, the rates of these three separate steps are equal at steady state, and (see notations in appendix)

$$\underset{\text{G/L mass transfer}}{r = k_l \cdot a \cdot (C_i - C_l)} = \underset{\text{L/S mass transfer}}{k_s \cdot a_s \cdot (C_l - C_s)} = \underset{\text{overall grain reaction.}}{m \cdot \eta \cdot k \cdot \Theta_{H_2} \cdot \Theta_{DPDS}} \quad (1)$$

For low pressure hydrogenation reactions, hydrogen is very often the "limiting reactant" due to its low concentration around the catalyst by comparison to the organic substrate. Assuming a first order Langmuir–Hinshelwood kinetic with respect to hydrogen at the particle surface ($\Theta_{H_2} = K_H C_s$), the elimination of C_l and C_s in (1) leads to the following equation:

$$C_i/r = 1/(k_l \cdot a) + 1/(m \cdot \eta \cdot k \cdot K_H \cdot \Theta_{DPDS}) + 1/(k_s \cdot a_s). \quad (2)$$

In Eq. (2), a and a_s are respectively the G/L and L/S interfacial areas, a_s being directly proportional to the catalyst weight m ($a_s = \lambda \cdot m$). Equation (2) could be rewritten as

$$1/r = 1/(C_i \cdot k_l \cdot a) + 1/C_i \cdot m \cdot [1/(\eta \cdot k') + 1/(\lambda \cdot k_s)] \quad (3)$$

with $k' = k \cdot K_H \cdot \Theta_{DPDS}$ (kinetic constant).

Equation (3) is useful to evaluate the importance of the G/L mass transfer. As a matter of fact, according to this model, the plot of $1/r$ as a function of $1/m$ should be a

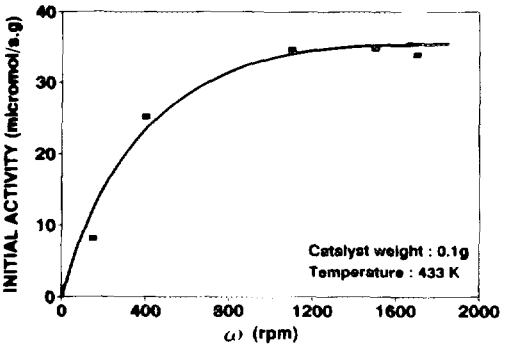

FIG. 2. Influence of the stirring rate on the initial activity ($NiMo/Al_2O_3$ catalyst).

straight line whose intercept gives the value of the G/L mass transfer constant k_m ($k_m = C_i \cdot k_1 \cdot a$). Furthermore, if both intraparticle and L/S mass transfer resistances are negligible (e.g., $\eta \approx 1$ and $k_s \gg k'$), the slope of the same plot provides the value of the kinetic constant $k_r = C_i \cdot k'$. This model was used to determine the experimental conditions allowing to perform the catalytic test under chemical control. To carry out these preliminary studies, a commercial NiMo catalyst was chosen.

E. Influence of the Stirring Rate

The influence of the stirring rate on the overall rate of the reaction was examined in order to estimate external mass transfer effects. Catalytic runs were conducted at 433 K under a hydrogen pressure of 3×10^5 Pa and with a catalyst weight of 0.1 g. Tests were carried out for various stirring rates ω ranging from 150 to 1700 revolutions per minute (rpm). The plot of the initial rate r_0 as a function of ω is shown in Fig. 2. The obtained curve presents a classical trend and shows that r_0 increases with ω for low stirring rates ($\omega < 1000$ rpm in this case) and reaches a plateau for higher rates ($\omega > 1000$ rpm), indicating that r_0 becomes independent of stirring. This behaviour means that below 1000 rpm, the rate of the reaction is limited by the external mass transfers (G/L and L/S), whereas above 1000 rpm the reaction rate is free of L/S mass transfer control.

F. Influence of the Catalyst Weight

Different catalytic tests were carried out with a catalyst loading between 0 and 0.32 g, under standard reaction conditions ($T = 433$ K, $P_{H_2} = 3 \times 10^5$ Pa). From the above study, the stirring rate was set to $\omega = 1500$ rpm. The variation of r_0 with the catalyst weight is illustrated in Fig. 3. This plot evidences that in the range 0–0.12 g, r_0 is directly proportional to m (slope: 35×10^{-6} mol $\cdot$ s$^{-1} \cdot$ g^{-1}), whereas for higher catalyst loading, this is obviously not the case. For instance, the initial specific activity calculated from the run with 0.324 g is only about 25×10^{-6} mol $\cdot$ s$^{-1} \cdot$ g^{-1} (e.g., 70% of the specific activity measured with a catalyst weight lower than 0.120 g). This emphasizes that for high catalyst weight, G/L mass transfer tends to limit the reaction rate, as appears clearly from Eq. (3). For very high values of m, the expression of r is reduced to

$$r = C_i \cdot k_1 \cdot a. \qquad (4)$$

According to (4) the curve of Fig. 3 should reach a plateau. However, this is difficult to observe experimentally due to the high catalyst loading required, and only a deviation from the straight line is obtained.

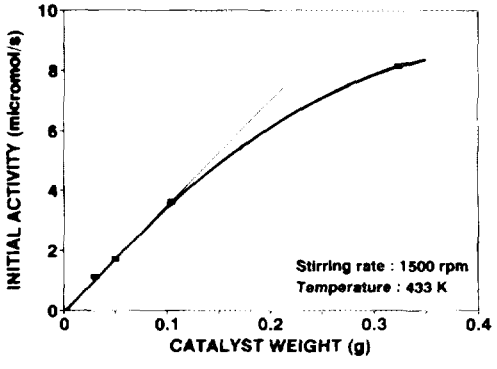

FIG. 3. Influence of the catalyst weight on the initial activity ($NiMo/Al_2O_3$ catalyst).

G. Intraparticle Mass Transfer Resistance

One way of evaluating the importance of intraparticle mass transfer resistance is to calculate the experimental Thiele modulus Φ (*43*) given by

$$\Phi = R^2 \cdot r_0 \cdot \rho / D \cdot C_s. \qquad (5)$$

Three different methods (Wilke-Chang, Tyn and Calus, or Hayduk and Minhas) (*44*) were used for the estimation of the diffusion coefficient D of the reactants. The calculated values being very close (within 5%) whatever the method employed, only the average one has been reported in Table 2. According to the above experimental results, the external mass transfer limitations may be avoided at $T = 433$ K and for $p_{H_2} = 3 \times 10^5$ Pa, $m = 0.100$ g, and $\omega = 1500$ rpm. Therefore, the concentrations at the L/S interface C_s can be taken as equal to C_l. For hydrogen, this concentration was determined by calculating its solubility in *n*-dodecane according to the equations of Prausnitz and Shair (*45*) and Radhakrishnan *et al.* (*46*). Table 2 summarizes the results obtained and gives the values of the Thiele moduli for hydrogen and DPDS. The effectiveness factor η can be determined from these values, by comparison with theoretical $\eta = f(\Phi)$ curves (*43*). For such low values of Φ, η is very close to 1, which means that intraparticle mass transfer resistance is negligible. Experimentally, the catalytic activity of two catalysts having 30 or 100 μm particle sizes were the same (35×10^{-6} mol/s · g), as expected from the theoretical calculation of the effectiveness factors.

TABLE 2

Diffusion Coefficients, Bulk Concentrations, and Thiele Moduli for H_2 and DPDS for DPDS Reduction ($T = 433$ K, $P_{H_2} = 3$ bar, $\omega = 1500$ rpm)

Reactant	D ($m^2 \cdot s^{-1}$)	C_s ($mol \cdot m^{-3}$)	Thiele modulus Φ
H_2	1.6×10^{-8}	50	0.07
DPDS	5.1×10^{-9}	300	0.04

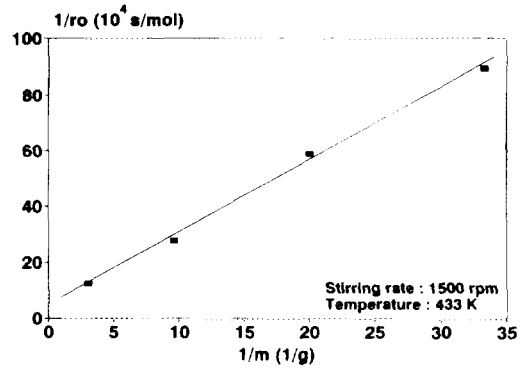

FIG. 4. Verification of the Alcorn and Sullivan model ($NiMo/Al_2O_3$ catalyst).

H. Determination of the G/L Mass Transfer Constant and the Kinetic Constant

The above studies of the influence of the stirring rate and of the catalyst weight on the initial rate of reduction of DPDS evidence that for $\omega > 1000$ rpm and $m < 0.120$ g, the reaction rate is not limited by external mass transfers (G/L and L/S). Furthermore, it was shown that there is no intraparticle mass transfer limitation. According to these conclusions, $\eta \approx 1$ and $k_s \gg k'$ and (3) may be simplified to the Alcorn and Sullivan model

$$1/r = 1/k_m + 1/(m \cdot k_r) \qquad (6)$$

with

$k_m = C_i \cdot k_l \cdot a$ (G/L mass transfer constant)

$k_r = C_i \cdot k'$ (kinetic rate constant).

The plot of $1/r_0$ as a function of $1/m$ is shown in Fig. 4. As expected, a straight line is obtained showing that the above model fits with experimental observations. Then the values of k_m and k_r can be deduced from the intercept and the slope of this straight line, giving

$$k_r = 39 \times 10^{-6} \text{ mol} \cdot \text{s}^{-1} \cdot \text{g}^{-1}$$

$$k_m = 23 \times 10^{-6} \text{ mol} \cdot \text{s}^{-1}.$$

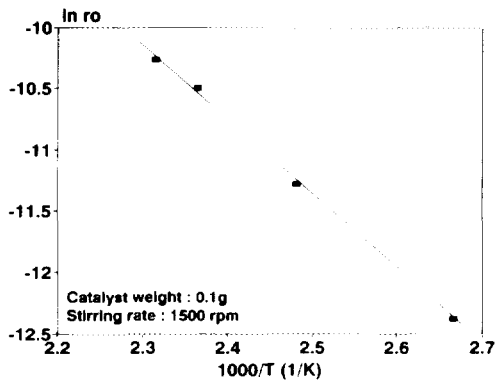

FIG. 5. Arrhenius diagram for the reduction of diphenyldisulfide into benzethiol ($NiMo/Al_2O_3$ catalyst).

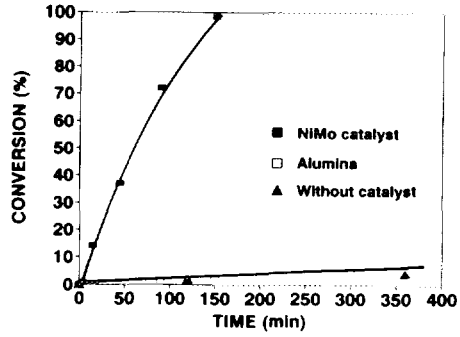

FIG. 6. Evolution of the conversion versus time for a NiMo catalyst, the alumina support, and without any catalyst.

These values demonstrate that under the reaction conditions used in this study, the G/L mass transfer proceeds much faster than the chemical reaction rate r_0, for $m \leq 0.1$ g ($r_0 = k_r \cdot m < 4 \times 10^{-6}$ mol · s^{-1}).

I. Influence of the Reaction Temperature

The influence of the temperature on the rate of the reduction of DPDS was studied in the range 373–433 K. The results observed are summarized in Fig. 5, which represents the Arrhenius diagram ($\ln r_0 = f(1/T)$) for this reaction. The apparent activation energy is close to 12 kcal · mol^{-1}. In this temperature range, the reaction is 100% selective toward thiophenol formation, whatever the conversion. The kinetic curve (conversion = $f(t)$) at 433 K is given on Fig. 6. In this figure the kinetic curves observed without catalyst or with alumina alone are also reported. These results indicate that at this temperature there is no thermal reaction (or catalysis by the wall of the reactor) and that alumina is inactive.

J. Influence of the Nature of the Catalyst

Examples of the variations of the conversion as a function of time for some catalysts are given on Fig. 7. It can be seen in this figure that the initial specific activities can be calculated from the first points of the kinetic curves measured after 15 min since the tangent to the curves at the origin and the chord are merged into one another for low conversions. The initial specific activities (r_0) of the various catalysts are given in Table 3 in which the activity of the nonsulfided NiMo catalyst as well as that of the support itself are also reported. These activities are much lower than that of the sulfided NiMo (more than 100 times smaller). In fact, the reaction rates observed in these two experiments do not differ significantly from a blank test, i.e., without any catalyst. This shows clearly that the active phase has to be a sulfide to perform the conversion of diphenyldisulfide. Another general conclusion valid for all the catalysts is that the reaction is 100% selective toward the formation of benzenethiol. No secondary prod-

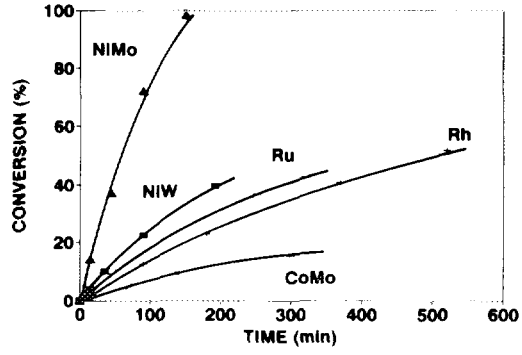

FIG. 7. Conversion of diphenyldisulfide as a function of time for some supported sulfided catalysts (catalyst weight = 0.10 g except Rh = 0.12 g).

TABLE 3

Specific Initial Activities r_0 for the Various Sulfided Catalysts Supported on Alumina, the Support Itself, and a Nonsulfided NiMo Sample

M	r_0 (10^{-6} mol/s · $g_{catalyst}$)
Ni	0.2
Co	1.0
Mo	1.6
W	0.8
Ru	9.9
Rh	5.0
NiMo	35.0
NiW	15.0
CoMo	3.0
Al_2O_3	0.2
NiMo oxide	0.2

ucts are observed in these reactions conditions.

The activities of the various sulfided catalysts vary in a wide range as deduced from the results given in Table 3 and schematized in Fig. 8a. The hydrotreating catalysts promoted by nickel, i.e., NiMo and NiW, are the most active for this reaction. The sulfides of ruthenium and rhodium present an intermediate activity while the others are more than 10 times less active. The synergetic effect observed in conventional hydrotreating reactions (hydrodesulfurization, hydrogenation of aromatics) for the catalysts containing molybdenum or tungsten is particularly important in the present case for the nickel promoted catalysts (20 times) but very small for the CoMo catalyst.

Even if it is difficult to make valid comparisons with other more conventional hydrogenation reactions, i.e., the hydrogenation of aromatics, since the experimental conditions are different (gas phase or liquid phase, temperature, hydrogen pressure) it seems that the general tendencies does not differ strikingly. Some data concerning biphenyl hydrogenation on the same catalysts drawn from our previous studies are reported on Fig. 8b. For both reactions the nickel promoted catalysts are the most active although in the reverse order (the NiW is more active than the NiMo in biphenyl hydrogenation). The CoMo does not present high hydrogenating performance as generally observed and the ruthenium sulfide catalyst possesses an intermediate activity. This leads to the assumption that active sites of comparable nature should be involved in both types of reactions.

K. TPR and TPD Results

Literature data suggest that for lamellar sulfides the active sites for hydrogenation and hydrodesulfurization reactions are coordinatively unsaturated cations. This conclusion was extended by us to other sulfides such as ruthenium sulfide and it was shown that the hydrogenation properties can be enhanced by hydrogen treatment due to an increase of the number of coordinatively un-

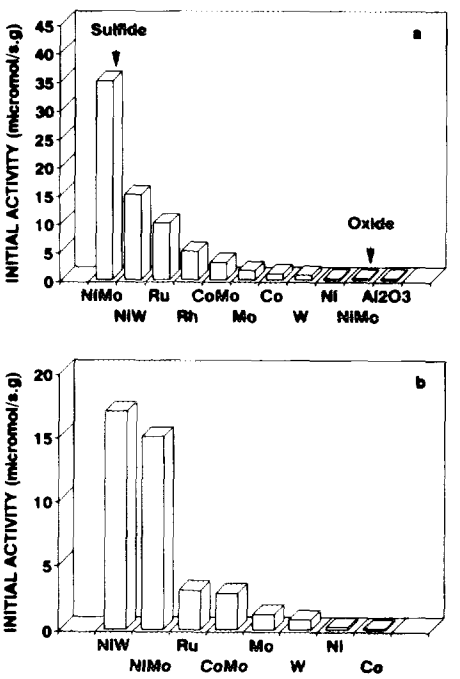

FIG. 8. Comparison of the properties of the supported catalysts (a) for the conversion of diphenyldisulfide; (b) for the conversion of biphenyl (533 K, P_{total} = 23 × 10^5 Pa, $P_{biphenyl}$ = 8 × 10^2 Pa, P_{H_2S} = 4 × 10^2 Pa).

saturated cations (*47*). In order to see if such sites can be involved in the hydrogenation of diphenyldisulfide two series of experiments were performed. The objective of the first set of experiments was to examine if vacancies can be formed in these low temperature conditions. The TPR results schematized in Fig. 9 show that all the catalysts do lose sulfur below 433 K (which temperature is represented by the vertical line on Fig. 9). For comparison purpose, three unsupported catalysts, i.e., RuS_2, MoS_2, and NiMoS (with the same atomic ratio Ni/(Ni + Mo) = 0.3 as the supported one) were also studied. The first one loses an important amount of sulfur below 433 K, MoS_2 loses a small quantity, and higher temperatures are required for NiMoS. These sulfur removals and the catalytic activities are reported in Table 4. It can be seen that all the catalysts which lose sulfur in the low temperature range are active for the conversion of diphenyldisulfide. By contrast, unsupported MoS_2 and NiMoS are inactive. It should be underlined that these two samples present the expected hydrogenation properties for biphenyl hydrogenation. Therefore, it appears that even if there is no direct correlation between the amount of sulfur evolved at the reaction temperature and the catalytic activity, the ability of the catalyst to form sulfur vacancies under these conditions is necessary for the catalytic activity.

TABLE 4

Amount of Sulfur Evolved under Hydrogen at the Reaction Temperature and Catalytic Activities

Catalyst	Amount of sulfur evolved below 433 K (10^{-6} mol/g)	Initial specific activity (10^{-6} mol/s · g)
Supported NiMo	390	35
Supported NiW	300	15
Supported Ru	450	10
Supported Rh	760	5
Supported CoMo	340	3
Supported Mo	220	1.5
Unsupported Ru	1500	20
Unsupported Mo	190	<1
Unsupported NiMo	15	<1

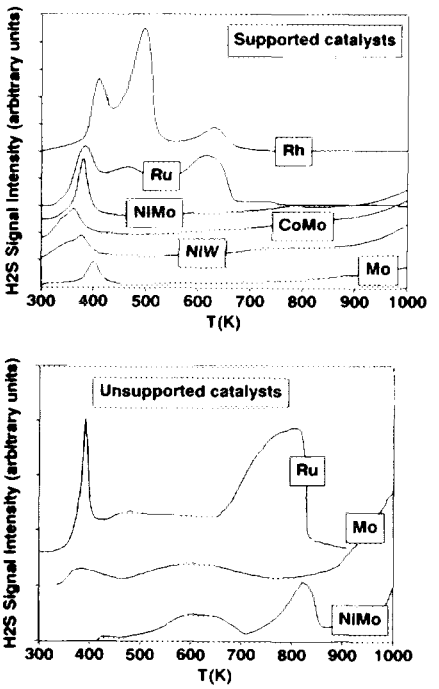

FIG. 9. Temperature programmed reduction of sulfide catalysts supported on alumina or unsupported.

In a second series of experiments the influence of hydrogen pretreatment on the catalytic activity was examined. To do that the test procedure was slightly modified. At room temperature, the catalyst was introduced into the reactor with the solvent but without the reactant. The reactor was flushed by nitrogen and heated to the desired pretreatment temperature. Nitrogen was replaced by hydrogen and left for 2 h at 473 K or 573 K under stirring. After these treatments, the reactor was cooled down to room temperature under hydrogen and flushed under nitrogen. The reactant was introduced and the typical test procedure was then used. In these conditions, the specific activity of a sulfided supported NiMo catalyst was 85 $\times$ 10^{-6} mol s^{-1} g^{-1} after treatment at 473 K and 40 after treatment at 573 K by comparison to 35 without pretreatment. It

should be underlined that the selectivity was not modified by these treatments.

At the end of the sulfidation process (see Scheme 1a), the surface is fully saturated with sulfur, either SH groups or bridged sulfur (*48*). A treatment under hydrogen at a medium temperature brings about the removal of the most labile sulfur anions and the formation of coordinatively unsaturated cations (Scheme 1b). On this kind of surface, hydrogen can be adsorbed in two forms, i.e., linked to the transition metal cation (*M*–H species) and to sulfur as SH groups, respectively $H^{\delta-}$ and $H^{\delta+}$ (*47–49*). At higher temperatures, a more drastic sulfur removal occurs and more numerous hydrogen adsorbed species are of the *M*–H form (Scheme 1c). Such modifications of the surface have been demonstrated by us in the case of ruthenium sulfide catalysts (*49*).

Therefore, according to the temperature of the reducing treatment, the number of coordinatively unsaturated cations is changed, but also the nature of the adsorbed species is not identical. Particularly, it should be noted that the amount of SH groups is modified, which species could play a role in this kind of reaction. As a matter of fact, in a homogeneous catalysis study of the same reaction with molybdenum–sulfur complexes, Coucouvanis (*50*) has suggested that the breakage of an S–S bond involves two SH groups according to the mechanism taken from Ref. (*50*) and given in Scheme 2.

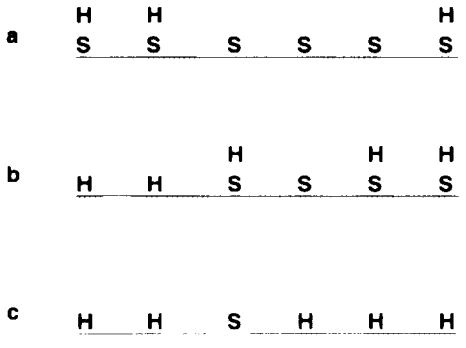

SCHEME 1

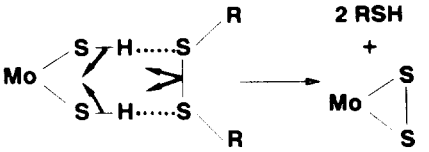

SCHEME 2

To determine, at the reaction temperature, the nature and the concentration of adsorbed species, the following experiments were performed using the TPR setup described in the experimental section for some of the most active catalysts (NiMo, NiW, CoMo, and Ru). The catalysts were flushed under nitrogen and heated in the same atmosphere up to 433 K. Then hydrogen was introduced for 15 min (time corresponding to the first determination of the conversion). After cooling down to room temperature under hydrogen, a flash heating of the solid to 573 K was performed under nitrogen to desorb the species present on the surface. The desorption profiles of hydrogen are given in Fig. 10. The obtained TPD profiles (dotted lines) evidence that at least two types of hydrogen species are adsorbed at the surface of the reduced catalysts which are differentiated by their temperatures of desorption. In order to quantify the amount of each adsorbed species, a mathematical simulation of the experimental curves has been carried out assuming a Gaussian distribution of both population of adsorbed species (*51–52*). As shown in Fig. 10, the simulated curves (solid lines) fit fairly well with the experimental ones. According to this, the total amount Q_t of hydrogen desorbed, as well as the amounts corresponding to the low temperature peak (denoted H^1) and the high temperature peak (H^2), can be easily calculated by integration. Results are reported in Table 5. The amounts of H_2S evolved from the surface detected by the UV photoionization detector are also given in Table 5. The comparison of these data to the specific activities show that no relation

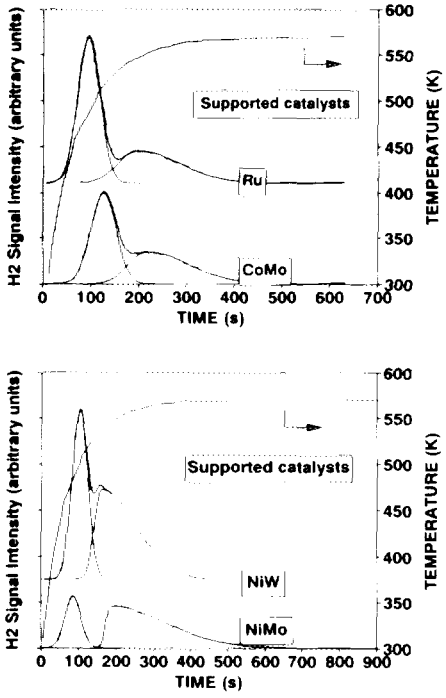

FIG. 10. Hydrogen thermodesorption profiles: dotted lines, experimental curves; solid lines, mathematical decomposition of the experimental curves.

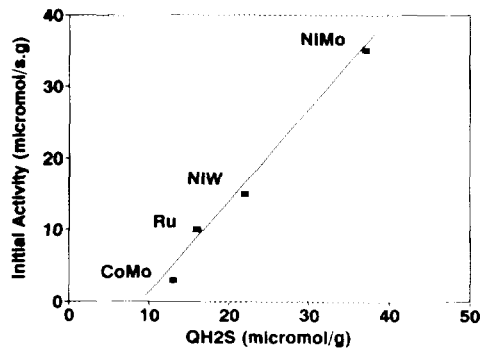

FIG. 11. Catalytic activities of some supported catalysts as a function of the amount of H_2S evolved.

can be found between the amount of hydrogen adsorbed, either the total amount or H^1 and H^2. By contrast, the catalysts can be ranked in the same order, taking into account the catalytic activities and the amount of H_2S. A satisfactory relationship is found between these two sets of data (Fig. 11). Considering that the evolved H_2S observed during the TPD accounts for the presence of surface sulfhydril groups, this result suggests that these groups play a role in the catalytic mechanism. The fact that there is not a direct relationship between the activity and the amount of desorbed H_2S suggests either that the catalytic sites also contain other entities or that not all the SH groups are involved in the catalytic mechanism. The first hypothesis is supported by the above conclusions on the influence on the catalytic properties of the presence of coor-

TABLE 5

Amount of H_2 and H_2S Desorbed after a H_2 Treatment at 433 K and Catalytic Activities

Catalyst	Amount desorbed (10^{-6} mol/g)		Specific activities (10^{-6} mol/s · g)
	H_2	H_2S	
NiMo	Q_t = 59	37	35
	H^1 = 14 H^2 = 45		
NiW	Q_t = 110	22	15
	H^1 = 40 H^2 = 70		
Ru	Q_t = 174	16	10
	H^1 = 119 H^2 = 55		
CoMo	Q_t = 130	13	3
	H^1 = 75 H^2 = 55		

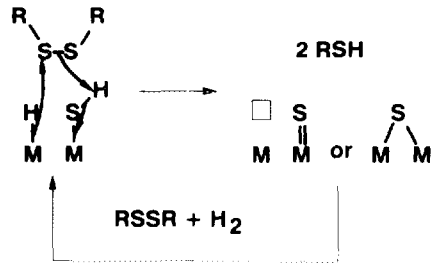

SCHEME 3

dinatively unsaturated cations and therefore appears more likely than the second one. Consequently, it can be proposed that the reaction proceeds according to Scheme 3.

Such a mechanism with a simultaneous occurrence of vacancies (leading to *M*–H) and SH groups is comparable to the one proposed by Angelici and co-workers for the hydrodesulfurization of thiophene (*53*, *54*). Kasztelan (*55*), in a descriptive model of surface sites on MoS_2 (WS_2) particles suggested also that both *M*–H and SH groups intervene in the hydrogenation reaction mechanism. Furthermore, experimental evidence of reactivity hydride species was given recently for ruthenium sulfide (*49*).

CONCLUSIONS

This work has evidenced that sulfide catalysts can achieve the catalytic reduction of diphenyldisulphides into their corresponding aromatic mercaptans at low temperature, at low hydrogen partial pressure, and in a G/L/S reactor. Preliminary studies related to the hydrodynamic characteristics of the reactor have made it possible to identify convenient experimental parameters that make it possible to conduct the reaction under chemical control. Under these conditions the catalytic properties of various solids (NiMo, CoMo, NiW, Mo, . . .) have been determined. To sum up these results, the activity of these systems varies in a wide range, the most active catalyst being the supported NiMo sample. Moreover, the selectivity toward formation of the desired products was 100% independent of the nature of the studied solid. TPR and TPD results strongly suggest the concomitant importance of both coordinatively unsaturated metal ions and SH groups on the catalytic activity. According to these data a tentative mechanism involving both SH and *M*–H species is proposed.

In order to improve this proposal, the reactivity of parasubstituted diphenyldisulfides has been examined to get information about the factors which could affect the reducibility of the S–S bonds. The results will be given in another paper.

APPENDIX: NOTATION

r	measured reaction rate
C_i	H_2 concentration at the G/L interface
C_s	H_2 concentration at the L/S interface
C_l	H_2 concentration in the liquid phase
$k_l \cdot a$	volumetric G/L transfer constant
$k_s \cdot a_s$	volumetric L/S transfer constant
a	G/L interfacial area per unit of volume
a_s	L/S interfacial area per unit of volume
m	catalyst weight
η	effectiveness factor
k	rate constant
ω	stirring rate
R	catalyst particle radius
D	diffusion coefficient
Φ	Thiele modulus
ρ	catalyst density
K_H	Langmuir–Hinshelwood adsorption constant for hydrogen
Θ_{DPDS}	fraction of surface covered by the substrate
Θ_{H_2}	fraction of surface covered by H_2

ACKNOWLEDGMENT

The authors thank ELF-AQUITAINE for Financial support.

REFERENCES

1. Weisser, O., and Landa, S., "Sulphide Catalysts: Their Properties and Applications." Pergamon, Oxford, 1973.

2. Mauchaussé, C., Mozzanega, H., Turlier, P. and Dalmon, J. A., *in* "Proceedings of the Ninth International Congress on Catalysis, Calgary, 1988" (M. J. Phillips and M. Ternan Eds.) Vol. 2, p. 755. Chem. Inst. of Canada, Ottawa, 1988.
3. Santiesteban, J. G., Bogdan, C. E., Herman R. G., and Klier, K., *in* "Proceedings of the Ninth International Congress on Catalysis, Calgary, 1988" (M. J. Phillips and M. Ternan, Eds.), Vol. 2, p. 561. Chem. Inst. of Canada, Ottawa, 1988.
4. Smith, K. J., Herman, R. G., and Klier, K., *Chem. Eng. Sci.* **45**(8), 2639 (1990).
5. Onopchenko, A., Sabourin, E. T., and Selwitz, C. M., *J. Org. Chem.* **44**(21), 3671 (1979).
6. Onopchenko, A., Sabourin, E. T., and Selwitz, C. M., US Patent 4,219,679 (1978). [To Gulf RED]
7. Braden, R., Kaupfe, H., and Hartung, S., US Patent 4,002,673 (1977). [To Bayer Aktiengesellschaft]
8. Moreau, C., Saens, C., Geneste, P., Breysse M., and Lacroix, M., *in* "Heterogeneous Catalysis and Fine Chemicals, II" (M. Guisnet *et al.*, Eds.), Studies in Surface Science and Catalysis, Vol. 59, p. 121. Elsevier, Amsterdam, 1991.
9. Malz, R. E., and Greenfield, H., *in* "Heterogeneous Catalysis and Fine Chemicals, II" (M. Guisnet *et al.*, Eds.), Studies in Surface Science and Catalysis, Vol. 59, p. 351. Elsevier, Amsterdam, 1991.
10. Koshelev, S. M., Mashkina, A. V., and Pauskshtis, E. A., *React. Kinet. Catal. Lett.* **44,** 367 (1991).
11. Koshelev, S. M., Pauskshtis, E. A., Verkhoturova, N. A., and Mashkina, A. V., *React. Kinet. Catal. Lett.* **29,** 376 (1988).
12. Lacroix, M., Marrakchi, H., Calais, C., Breysse, M., and Forquy, C., *in* "Heterogeneous Catalysis and Fine Chemicals, II" (M. Guisnet *et al.*, Eds.), Studies in Surface Science and Catalysis, Vol. 59, p. 217. Elsevier, Amsterdam, 1991.
13. Forquy, C., Lacroix, M., and Breysse, M., French Patent 90 10762 (1990). [To Société Nationale ELF Aquitaine (Production)]
14. Forquy, C., and Arretz, E., *in* "Heterogeneous Catalysis and Fine Chemicals, I" (M. Guisnet *et al.*, Eds.), Studies in Surface Science and Catalysis, Vol. 41, p. 91. Elsevier, Amsterdam, 1988.
15. Sakurada, A., and Hirowatari, N., Japanese Patent 80 36,409 (1980). [To Mitsubishi Petrochemical Co.]
16. Sakurada, A., and Hirowatari, N., Japanese Patent 80 15,413 (1980). [To Mitsubishi Petrochemical Co.]
17. Sherk, F. T., and Kubicek, D. H., US Patent 3,799,989 (1974). [To Phillips Petroleum Co.]
18. Voronkov, M. G., Deryagina, E. N. Klochkova, L. G., Savushkina, V. I., and Chernishev, E. A., *Zh. Org. Khim.* **11**(5), 1132 (1975).
19. Ivanova, G. M., Voronova, L. K., Deryagina, E. N., and Voronkov, M. G., *Zh. Org. Khim.* **15**(6), 1232 (1979).
20. Sukhomaz, E. N., Deryagina, E. N., and Voronkov, M. G., *Zh. Org. Khim.* **16**(2), 472 (1980).
21. Laufer, R. J., German Patent 1 816 477 (1969). [To Consolidation Coal Co.]
22. Mariotti, J. F., Blanc, J., and Thibault, C., French Patent 2 218 330 (1973). [To Société Nationale des pétroles d'Aquitaine]
23. Pitt, H., US Patent 2,947,788, (1960). [To Stauffer Chemical]
24. Pitt, H., German Patent 1,939,468, (1970). [To Stauffer Chemical]
25. Fujimori, K., Togo, H., and Oae, S., *Tetrahedron Lett.* **21**(51), 4921 (1980).
26. Oae, S., and Togo, H., *Bull. Chem. Soc. Jpn.* **56**(12), 3802 (1983).
27. Knusli, E., *Gazz. Chim. Ital.* **79,** 621 (1949).
28. Wagner, A., *Chem. Ber.* **99**(1), 375 (1966).
29. Yamashita, H., and Takahashi, Y., Japanese Patent 74 25,255 (1974). [To Sugai Chemical Industry Co.]
30. Hokko Chemical Industry Co., Japanese Patent 83 188,854 (1983).
31. Brown, H. C., Nazer, B., and Cha, J. S., *Synthesis* **6,** 498 (1984).
32. Krishnamurthy, S., and Aimino, D., *J. Org. Chem.* **54,** 4458 (1989).
33. Ookawa, A., Yokohama, S., and Soai, K., *Synth. Commun.***16**(7), 819 (1986).
34. Overman, L. E., Matzinger, D., O'Connor, E. M., and Overman, J. D., *J. Am. Chem. Soc.* **96**(19), 6081 (1974).
35. Happer, D. A., Mitchell, J. W., and Wright, G. J., *Aust. J. Chem.* **26,** 121 (1973).
36. Overman, L. E., and Petty, S. T., *J. Org. Chem.* **40**(19), 2779 (1975).
37. Woods, T. S., and Klayman, D. L., *J. Org. Chem.* **39**(25), 3716 (1974).
38. Maiti, S. N., Spevak, P., Singh, M. P., Micetich, R. G., and Narender Reddy, A. V., *Synth. Commun.* **18**(6), 575 (1988).
39. Maiti, S. N., Singh, M. P., Spevak, P., Micetich, R. G., and Narender Reddy, A. V., *J. Chem. Res. Synop.* **1,** 256 (1988).
40. Lacroix, M., Boutarfa, N., Guillard, C., Vrinat, M., and Breysse, M., *J. Catal.* **120,** 405 (1989).
41. Vrinat, M., Lacroix, M., Breysse, M., and Fréty, R., *Bull. Soc. Chim. Belg.* **93**(8–9), 697 (1984).
42. Rushton, J. H., Costlich, E. W., and Everett, H. J., *Chem. Eng. Prog.* **46,** 395 (1950).
43. Satterfield, C. N., *in* "Mass Transfer in Heterogeneous Catalysis." M.I.T. Press, Cambridge, MA, (1970).
44. Reid, R. C., Praussnitz, J. M., and Poling, B. E., *in* "The Properties of Gases and Liquids," fourth ed. McGraw–Hill, New York, 1986.

45. Prausnitz, J. M., and Shair, F. H., *AIChE J.* **7,** 682 (1961).
46. Radhakrishnan, K., Ramachandran, P. A., Brahme, P. H., and Chaudari, R. V., *J. Chem. Eng. Data* **28,** 1 (1983).
47. Lacroix, M., Mirodatos, C., Breysse, M., Decamp, T., and Yuan, S., *in* "Proceedings, 10th International Congress on Catalysis, Budapest, 1992" (L. Guczi, F. Solymosi, and P. Tetenyi, Eds.), Vol. A, p. 597. 1992.
48. Wambeke, A., Jalowiecki, L., Kasztelan, S., Grimblot, J., and Bonnelle, J. P., *J. Catal.* **109,** 320 (1988).
49. Lacroix, M., Yuan, Y., Breysse, M., Dorémieux-Morin, C., and Fraissard, J., *J. Catal.* **138,** 409 (1992).
50. Coucouvanis, D., Hadjikyriacou, A., Draganjac, M., Kanatzidis, M. G., and Ileperuma, O., *Polyhedron* **5**(1/2), 349 (1986).
51. Geantet, C., Calais, C., and Lacroix, M., *C.R. Acad. Sci. Paris* **315**(2), 439 (1992).
52. Tonge, K. H., *Thermochim. Acta* **74,** 151 (1984).
53. Markel, E. G., Shrader, G. L., Sauer, N. N., and Angelici, R. J., *J. Catal.* **116,** 11 (1989).
54. Sauer, N. N., Markel, E. J., Schrader, G. L., and Angelici, R. J., *J. Catal.* **117,** 295 (1989).
55. Kasztelan, S., *Langmuir* **6,** 590 (1990).